THE JOURNAL OF PHYSICAL CHEMISTRY A

 VOLUME 113, NUMBER 51, DECEMBER 24, 2009

ARTICLES

Steric Effect in the Energy Transfer Reaction of Oriented Kr ($^3P_2$, $M_J = 2$) + CO

H. Ohoyama,* K. Yasuda, and T. Kasai

Department of Chemistry, Graduate School of Science, Osaka University, Toyonaka, Osaka 560-0043, Japan

Received: August 4, 2009; Revised Manuscript Received: September 28, 2009

Atomic alignment effect for the formations of CO ($a'\ ^3\Sigma^+$) and CO ($d\ ^3\Delta$) in the energy transfer reaction of oriented Kr ($^3P_2$, $M_J = 2$) + CO has been measured at a collision energy of 0.07 eV. The emission intensities of CO ($a'\ ^3\Sigma^+$) and CO ($d\ ^3\Delta$) were similarly highly enhanced when the electron angular momentum of Kr ($^3P_2$) is aligned perpendicular to the relative velocity vector. We observed the analogous atomic alignment effect between the CO ($a'\ ^3\Sigma^+$) and CO ($d\ ^3\Delta$) formations. That is, the $|M_J'| = 2$ magnetic substate in the collision frame is significantly less reactive than the other M_J' states. In addition, the large difference of the cross section ($\sigma_\Sigma/\sigma_\Pi \approx 2.0$) between the Σ- and Π-configuration of the unpaired 4p orbital of Kr ($^3P_2$) is recognized.

1. Introduction

The reaction of Rg (^3P) + CO is an important as a benchmark system for the collisional energy transfer process,[1−4] and it is also an ideal system for studying the state selectivity in the collisional energy transfer process because there are many emitting excited states.

For the Kr ($^3P_2$) + CO reaction, the total quenching constant has been reported to be $k = 5.7 \times 10^{-11}$ cm^3 s^{-1} (10.5 Å^2),[5] which is smaller than the one (20 Å^2) predicted from the charge-transfer model via the $Kr^+ + CO^-$ ionic curve.[6] The outer valence electron configuration of Kr ($^3P_2$) is $4p^55s^1$. The excitation energy of Kr ($^3P_2$) is 9.92 eV. The excited states of CO that can be energetically accessible by the excitation energy of Kr ($^3P_2$) are the ($A\ ^1\Pi$, $a\ ^3\Pi$) states with the $(5\sigma)^1\ (1\pi)^4\ (2\pi)^1$ electron orbital configuration and the ($a'\ ^3\Sigma^+$, $e\ ^3\Sigma^-$, $d\ ^3\Delta$, $I\ ^1\Sigma^-$, $D\ ^1\Delta$) states in the $(5\sigma)^2\ (1\pi)^3\ (2\pi)^1$ configuration. Among these states, the following four reaction channels being in the near-resonant high vibrational levels (v) have been identified.[1]

$$Kr(^3P_2) + CO \rightarrow CO(d^3\Delta;\ v = 20-21) + Kr \quad (1a)$$

$$\rightarrow CO(a'\ ^3\Sigma^+;\ v = 23-26) + Kr \quad (1b)$$

$$\rightarrow CO(A\ ^1\Pi;\ v = 9-11) + Kr \quad (1c)$$

$$\rightarrow CO^*(\text{unassigned}) + Kr \quad (1d)$$

The branching fraction has been reported to be 0.24:0.23:0.23:0.30 for the reactions 1a−1d.[1] No formation of CO ($e\ ^3\Sigma^-$) has been reported. The emission spectrum from the Kr ($^3P_2$) + CO reaction has been reported within the wavelength region of 300−900 nm.[1] The emission from 320 to 380 nm has been assigned to the CO ($d\ ^3\Delta$) emission.[1,7] The CO ($a'\ ^3\Sigma^+$) emission has been assigned to be dominant at the wavelength region of 420−480 nm.[1] The emission from 520 to 900 nm has been assigned to the overlap of the emissions from three states, CO (a', d) and CO*. (One-third of the emissions are assigned to CO (a') and CO (d), and the rest are due to the unassigned CO*.)[1] The electron orbital configuration of the CO ($d\ ^3\Delta$) state

10.1021/jp907518u
Published on Web 12/01/2009

is represented by $(5\sigma)^2\ (1\pi)^3\ (2\pi)^1$. The CO ($a'\ ^3\Sigma^+$) state also has the same orbital configuration. That is, these two states are formed by the promotion of an electron from the 1π orbital to the 2π orbital.

It has been suggested that the Kr (^{3}P) + CO reaction proceeds via the direct curve crossings between the entrance and exit covalent surfaces.[1−4] If the Kr (^{3}P) + CO reaction proceeds via the direct curve crossing mechanism, the steric effect due to the electron exchange should be an important factor to control the reaction. However, the steric aspect in the title reaction has not been directly studied.

In the present study, the atomic alignment effects for the formations of CO ($a'\ ^3\Sigma^+$), CO ($d\ ^3\Delta$), and CO* were studied in the Kr ($^3P_2$) + CO reaction. The emission intensities of CO ($a'\ ^3\Sigma^+$), CO ($d\ ^3\Delta$), and CO* are highly enhanced when the electron angular momentum of Kr ($^3P_2$) is aligned perpendicular to the relative velocity vector.

2. Experiment

The experimental apparatus and procedures are almost the same with the previous one.[8,9] A metastable Kr ($^3P_{0,2}$) beam was generated by a pulsed glow discharge with a pulse width of 100 μs and then state-selected by a magnetic hexapole. The M_J state distribution of the state-selected Kr ($^3P_2$) beam was directly determined by separating each M_J state using a Stern−Gerlach type inhomogeneous magnetic state selector as a function of arrival time, t_0.[8,9] The state-selected metastable Kr ($^3P_2$) beam within the arrival time region ($1.92 \le t_0 \le 2.17$ ms) (corresponds to $v_s = 490 \pm 30$ ms^{-1}) is composed of almost pure Kr ($^3P_2$, $M_J = 2$). The emission signal within this time region is used for further study. An almost pure Kr ($^3P_2$, $M_J = 2$) beam collides with the CO beam in a homogeneous magnetic orientation field $\boldsymbol{B}$. In the present study, the Kr ($^3P_2$, $M_J = 2$) beam is oriented in the homogeneous magnetic orientation field $\boldsymbol{B}$. The CO beam was injected with a stagnation pressure of 10 Torr from a pulsed valve that is placed at a distance of 8 cm from the beam crossing point. The emission from CO ($a'\ ^3\Sigma^+$) (420−480 nm) was selectively collected through the suitable band-pass filters (HOYA, B390 & L42) and detected by a photomultiplier (Hamamatsu R943-02). The emission from the CO ($d\ ^3\Delta$) (320−380 nm) and from the three states of CO (a', d, CO*) (520−900 nm) were also measured through the suitable filters (HOYA, UV32 & U340, Y52). The signal from the photomultiplier was counted by a multichannel scaler (Stanford SR430). The emission intensities from CO ($a'\ ^3\Sigma^+$), CO ($d\ ^3\Delta$), and CO (a', d, CO*) were measured as a function of the direction of the magnetic orientation field in the laboratory frame (rotation angle Θ). The origin of Θ is the direction of the Kr ($^3P_2$) beam axis. The homogeneous magnetic orientation field was generated by the four pieces of ferrite magnet mounted on a motor-driven rotatable stage, and its direction $\boldsymbol{B}$ was rotated around the beam crossing point over the angle region $-40 \le \Theta \le 155°$ by an interval of 15°.

3. Results and Discussion

3.1. Atomic Alignment Effects in the Different Reaction Channels. Figure 1 shows the Θ-dependence of the emission intensities for CO ($a'\ ^3\Sigma^+$), CO ($d\ ^3\Delta$), and CO (a', d, CO*) in the Kr ($^3P_2$, $M_J = 2$) + CO reaction. The emission intensities are highly enhanced when the electron angular momentum of Rg ($^3P_2$) is aligned perpendicular to the relative velocity vector. Although the Θ-dependence in the CO ($d\ ^3\Delta$) channel is slightly moderate than that in the CO ($a'\ ^3\Sigma^+$) channel, the atomic alignment effects in the three channels, CO ($a'\ ^3\Sigma^+$), CO ($d\ ^3\Delta$), and CO*, are found to be fairly similar with each other.

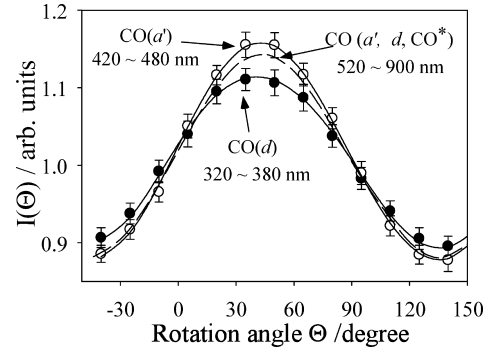

Figure 1. Emission intensities of the excited CO's in the Kr ($^3P_2$, $M_J = 2$) + CO reaction as a function of rotation angle Θ of the magnetic orientation field direction. Experimental: CO ($a'\ ^3\Sigma^+$) (open circle), CO ($d\ ^3\Delta$) (closed circle). Θ-dependence represented by the fitting with using eq 4: CO ($a'\ ^3\Sigma^+$) (solid solid line), CO ($d\ ^3\Delta$) (solid line), CO (a', d, CO*) (dashed line). The origin of the rotational angle Θ is the direction of the Kr ($^3P_2$) beam axis.

3.2. M_J'-Dependent Cross Section in the Collision Frame, $\sigma^{|M_J'|}$. In the present study, the Kr ($^3P_2$, $M_J = 2$) atomic beam is oriented in a homogeneous magnetic orientation field $\boldsymbol{B}$. For the collision processes, however, the relative velocity vector serves as the other relevant quantization axis. The cross section is then a function of the angle between those two quantization axes. In the following discussion, we use the notation of M_J for projections in the laboratory frame (the quantization axis is the magnetic orientation field $\boldsymbol{B}$). On the other hand, primed symbols such as M_J' are used for projections in the collision frame (the quantization axis is the relative velocity vector).

In order to extract the quantitative information on the steric effect, we accommodate the evolution procedure based on an irreducible representation of the density matrix. The detail of the analytical procedures and the derivation of all the algebra were reported elsewhere.[8] In general, the Θ-dependence of the emission intensity$I(\Theta)$ can be expressed by

$$I(\Theta) = \frac{D\bar{I}}{(2J+1)} \sum_{kq} g_k(J) S_{kq}(B,J) T_{kq}(B,J) \qquad (2)$$

where $S_{kq}(B,J)$ and $T_{kq}(B,J)$ are the real multipole moments of the density matrix of the prepared oriented Kr ($^3P_2$, $M_J = 2$) atom and of the collision density matrix, respectively, D is an experimental detection efficiency, $\bar{I}$ the polarization averaged cross section, and $g_k(J)$ are numerical factors. In the present study, the general eq 1 can be simplified as the following equation by using the relative cross section of each magnetic substate M_J' in the collision frame, $\sigma^{|M_J'|}$.

$$I(\Theta) = \frac{1}{280}(39\sigma^{M_J'=0} + 88\sigma^{|M_J'|=1} + 153\sigma^{|M_J'|=2}) + \frac{1}{16}(-3\sigma^{M_J'=0} - 4\sigma^{|M_J'|=1} + 7\sigma^{|M_J'|=2})\langle\cos(2(\Theta_{v_R} - \Theta))\rangle + \frac{1}{64}(3\sigma^{M_J'=0} - 4\sigma^{|M_J'|=1} + \sigma^{|M_J'|=2})\langle\cos(4(\Theta_{v_R} - \Theta))\rangle \qquad (3)$$

where $\Theta_{v_R} - \Theta$ is the angle between the direction of the orientation magnetic field $\mathbf{B}$ (Θ) and the direction of the relative velocity $v_R(\Theta_{v_R})$ in the laboratory coordinate. Since Θ_{v_R} has a distribution by the misalignment caused by the velocity distribution of CO beam, we must use the $\cos(2n(\Theta_{v_R} - \Theta))$ factors averaged over the Maxwell−Boltzmann velocity distribution of CO beam at room temperature, $\langle\cos(2n(\Theta_{v_R} - \Theta))\rangle$. This equation is equivalent to the general multipole moment's form

$$I(\Theta) = a_0 + a_2\langle\cos(2(\Theta_{v_R} - \Theta))\rangle + a_4\langle\cos(4(\Theta_{v_R} - \Theta))\rangle \quad (4)$$

The coefficients, a_n, were determined as the fitting parameters by the fitting of the experimental results in Figure 1 using eq 4 through a χ^2 analysis. They are summarized as follows.

CO(a'):

$$a_2/a_0 = -0.150 \pm 0.005, \quad a_4/a_0 = 0.003 \pm 0.006$$

CO(d):

$$a_2/a_0 = -0.110 \pm 0.006, \quad a_4/a_0 = -0.006 \pm 0.006$$

CO(a', d, CO*):

$$a_2/a_0 = -0.140 \pm 0.005, \quad a_4/a_0 = 0.001 \pm 0.006$$

The relative cross section for each M_J' substate in the collision frame, $\sigma^{|M_J'|}$, can be derived from eq 3 using a_n coefficients. The relative cross sections $\sigma^{|M_J'|}$ are determined as follows.

CO(a′):

$$\sigma^{M_J'=0}:\sigma^{|M_J'|=1}:\sigma^{|M_J'|=2} = 1:0.876 \pm 0.020:0.662 \pm 0.012$$

CO(d):

$$\sigma^{M_J'=0}:\sigma^{|M_J'|=1}:\sigma^{|M_J'|=2} = 1:1.022 \pm 0.029:0.775 \pm 0.018$$

CO(a', d, CO*):

$$\sigma^{M_J'=0}:\sigma^{|M_J'|=1}:\sigma^{|M_J'|=2} = 1:0.918 \pm 0.021:0.700 \pm 0.013$$

They were plotted in Figure 2. Although the M_J' dependence for the CO (d) formation is slightly moderate than that for the CO (a') formation, the M_J' dependences in every reaction channels are qualitatively similar. That is, the $|M_J'| = 2$ states are significantly less reactive than the other M_J' states.

3.3. Atomic Alignment Effect on the Energy Transfer Probability. If the energy transfer proceeds via the curve-crossing mechanism through an ionic-pair surface (Kr^+-CO^-), the clear atomic alignment effect constrains that the prepared configuration of the unpaired inner 4p orbital of Kr ($^3P_2$) must be conserved within the ionic pair (Kr^+-CO^-) during a long-duration time until the energy transfer is accomplished via the back electron transfer. In addition, three exit channels (CO (a'), CO (d), and CO*) should express the wildly divergent M_J' dependence because these exit channels compete with each other through the common ionic pair (Kr^+-CO^-) potential surface. On the other hand, if the Kr ($^3P_2$) + CO reaction proceeds via the direct curve crossings between the entrance and exit covalent surfaces,[2] the similar atomic alignment effect being observed in the three exit channels can be reasonably recognized as the similarity in the electron exchange process because the electron orbital configurations of CO (a') and CO (d) are commonly represented by $(5\sigma)^2\,(1\pi)^3\,(2\pi)^1$. Therefore, the clear and similar M_J' dependence being observed in the three exit channels strongly suggests that the Kr ($^3P_2$) + CO reaction proceeds via the direct curve crossing mechanism.

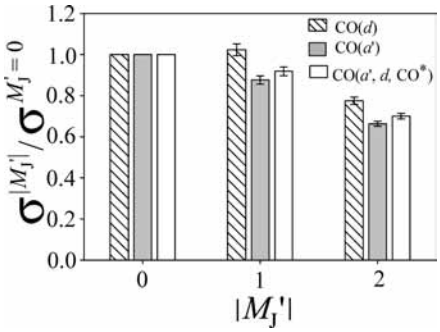

Figure 2. The relative cross section for each $|M_J'|$ state in the collision frame, $\sigma^{M_J'=0}$, $\sigma^{|M_J'|=1}$, and $\sigma^{|M_J'|=2}$. CO ($d\,^3\Delta$) (shaded bar), CO ($a'\,^3\Sigma^+$) (gray bar), CO (a', d, CO*) (white bar).

According to the electron exchange process, the energy transfer proceeds via the following two electron-transfer processes.

Process 1 Electron transfer (ET) from the 5s orbital of Kr ($^3P_2$) to the empty 2π orbital of CO.

Process 2 Back electron transfer (BET) from the 1π orbital of CO to the unpaired 4p orbital of Kr ($^3P_2$).

In order for the energy transfer to occur, the set of orbitals, ($4p + 1\pi$) and ($5s + 2\pi$), must overlap. A clear M_J' dependence being observed in the title reaction indicates that the configuration of the unpaired 4p atomic orbital gives a significant effect on the electron and/or the back-electron transfer processes.

3.3.1. Atomic Alignment Effect on the Entrance Potentials. First, we consider the atomic alignment effect on the entrance potentials. On the basis of the small total quenching cross section, the energy transfer should take place at a rather close intermolecular distance. At such close intermolecular distance, the open shell nature of the Kr^+ (^2P_j) ion core should give an important role on the effective adiabatic potentials. In other words, the electrostatic induction terms should contribute in the entrance potentials. In order to correctly understand the M_J' dependent process, it should be necessary to take into account the M_J' dependence of the entrance potentials due to the open shell nature of the Kr^+ (^2P_j) ion core.

The effective adiabatic potentials can be considered as the sum of three terms: V_{so}, spin−orbit; V_{rot}, centrifugal term; and V_{el}, electrostatic interaction, when only the fine structure states are introduced in the close coupling equations.[10] For Hund's cases (a) and (c), the explicit expressions of the effective adiabatic potential-energy curves following LS coupling with the small impact parameters have been formulated by Aquilanti et al.[10−12] At the intermediate distances (Hund's case c), the open shell character of the Kr^+ (^2P_j) ion core splits the entrance surface into three branches $V_{J\Omega}$, designated as V_{22}, V_{21}, V_{20}, that correlate with Kr ($^3P_2$, M_J') (Ω is the absolute projection of the total electronic angular momentum J along the intermolecular axis. In the present study, Ω directly tends to $|M_J'|$ at large intermolecular distance). The three effective adiabatic potentials $V_{J\Omega}$ have the different weight of Σ and Π characters.[11]

$$V_{J\Omega} = W_\Pi(J\Omega)V_\Pi + W_\Sigma(J\Omega)V_\Sigma \quad (5)$$

where W_Σ and W_Π are the weights of the Σ and Π characters in the $V_{J\Omega}$ entrance channels at each crossing point.

$$W_\Pi(2,2) = 1, \quad W_\Sigma(2,2) = 0$$
$$W_\Pi(2,1) = \frac{2}{3}\cos^2\alpha, \quad W_\Sigma(2,1) = 1 - \frac{2}{3}\cos^2\alpha \quad (6)$$
$$W_\Pi(2,0) = \sin^2\alpha', \quad W_\Sigma(2,0) = \cos^2\alpha'$$

where

$$\cos^2\alpha = \frac{1}{2} + \frac{3\beta_1}{10\left(1 + \frac{9}{25}\beta_1^2\right)^{1/2}}, \quad \beta_1 = V_2/\varepsilon_1$$

$$\cos^2\alpha' = \frac{1}{2} + \frac{1 - 9\beta_0/5}{4\sqrt{2}\{1 + [(1 - 9\beta_0/5)/2\sqrt{2}]^2\}^{1/2}}, \quad \beta_0 = V_2/\varepsilon_0$$

V_2 is the anisotropic component of the interaction that is obtained by a spherical harmonics expansion of the potential around the P-state atom, and ε is the spin−orbit energy separation in the ^3P_j atom (i. e., $\epsilon_0 = (^3P_0 - {}^3P_2) = 5220\ cm^{-1}$, $\epsilon_1 = (^3P_1 - {}^3P_2) = 945\ cm^{-1}$ for Kr ($^3P_2$)).

On the basis of this treatment, the relative reactivity for each magnetic substate in the collision frame, $\sigma^{|M_J'|}$, can be expressed as follows

$$\sigma^{|M_J'|} = W_\Pi(|M_J'|)\sigma_\Pi + W_\Sigma(|M_J'|)\sigma_\Sigma \tag{7}$$

where σ_Π and σ_Σ is the cross section for the Π and Σ character in the entrance channels $V_{J,\Omega=|M_J'|}$ at each curve crossing point, respectively. To accurately evaluate the $\sigma^{|M_J'|}$ cross sections, one has to know the accurate potential energy surface near each curve crossing point. However, the theoretical calculation of the potential surfaces is incredibly difficult for the present system; no such calculations presently exist. In order to roughly evaluate the atomic alignment effect on the entrance potentials, at this stage, we assumed that the crossing distance and the energy transfer probability for each Π and Σ character for each product channel is similar at each $V_{J\Omega}$ potential. If this is the case, the weight of Σ and Π characters, $W_\Pi(|M_J'|)$ and $W_\Sigma(|M_J'|)$, can be simply expressed by the common parameter V_2 (and/or β_1 and β_0). Therefore, the relative cross sections $\sigma^{|M_J'|}$ can be expressed by using the two parameters, V_2 and$R \equiv \sigma_\Sigma/\sigma_\Pi$. The parameters V_2 and R were determined by a least-squares fitting of the experimental relative cross sections $\sigma^{|M_J'|}$ using eq 7. The experimental $\sigma^{|M_J'|}$ can be well represented by using the following parameters

CO(a'):

$$(\beta_1 = V_2/\varepsilon_1 = 2.0), \quad \frac{\sigma_\Sigma}{\sigma_\Pi} = 2.0 \tag{8a}$$

CO(d):

$$(\beta_1 = V_2/\varepsilon_1 = 1.5), \quad \frac{\sigma_\Sigma}{\sigma_\Pi} = 1.7 \tag{8b}$$

Since the β_1 in reactions 1a and 1b are larger than unity, the curve crossings should occur at the rather short intermolecular distance where the anisotropic term gives an important role on the effective adiabatic potentials. This result should support the direct curve crossings between the covalent surfaces in the Kr ($^3P_2$) + CO reaction because the energy transfer must occur dominantly at a short distance.[2]

The calculated weights of the Π and Σ characters in the entrance channels at each crossing point, $W_\Pi(|M_J'|)$ and $W_\Sigma(|M_J'|)$, are summarized in Table 1. The repulsive nature (Π character) of the entrance potential increase in the order Ω = 0, 1, 2. A schematic drawing of the entrance surfaces is shown in Figure 3. The formation of the (d; v = 20−21) levels and the more endoergic a' levels might proceed via the most repulsive Ω = 2 potential. The other entrance channel potentials (Ω = 0, 1) must be sufficiently attractive to provide pathways for formation of the exoergic products. We can find the notable difference in both β_1 and σ_Σ/σ_Π between the CO (a') and CO(d) channels.

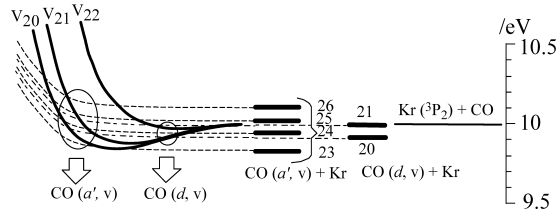

Figure 3. A schematic drawing of the energy transfer mechanism via the direct curve crossings between the entrance (solid lines) and exit covalent surfaces for CO (a' $^3\Sigma^+$, v = 23−26)) (dashed lines), CO (d $^3\Delta$, v = 20, 21) (dashed-dotted lines). The open shell character of the Kr^+ (^2P_j) ion core splits the entrance surface into three branches $V_{J\Omega}$, designated as V_{22}, V_{21}, V_{20}, that correlate with Kr ($^3P_2$, M_J'). For the interaction of a ^{3}P-state atom with a closed-shell particle, the repulsive nature of the entrance potential is known to increase in the order Ω = 0, 1, 2. The vibrational energy levels for each excited CO states were cited from ref 1 (bold lines).

TABLE 1: The Weights of the Π and Σ Characters, $W_\Pi(|M_J'|)$ and $W_\Sigma(|M_J'|)$, at the Crossing Points on the Effective Adiabatic Entrance Potentials (V_{22}, V_{21}, V_{20}) for the CO(a') and CO(d) Formations

	$W_\Sigma(0)/W_\Pi(0)$	$W_\Sigma(\|1\|)/W_\Pi(\|1\|)$	$W_\Sigma(\|2\|)/W_\Pi(\|2\|)$	σ_Σ/σ_Π
CO (a')	0.56/0.44	0.41/0.59	0/1	2.0
CO (d)	0.59/0.41	0.45/0.55	0/1	1.7

The smaller value of β_1 and σ_Σ/σ_Π for the CO (d) formation indicates that the CO (d) formation proceeds at the relatively longer intermolecular distance (and/or at the larger impact parameter). This result might be related to the Ω-level selectivity in the CO (d $^3\Delta_\Omega$) formation due to the angular momentum conservation because the theoretical study has suggested that the CO (d) formation occurs at the noncollinear collision geometries.[13]

3.3.2. Atomic Alignment Effect on the Electron Exchange. The large difference of the cross section between the Σ- and Π-configurations ($\sigma_\Sigma/\sigma_\Pi \approx 2.0$) indicates that the dynamics is significantly controlled by the configuration of the unpaired 4p orbital of Kr ($^3P_2$) in the collision frame. The observed steric effect,$\sigma_\Sigma/\sigma_\Pi \approx 2$, means that the Σ-configuration is 2 times more reactive than the Π-configuration. In order to understand the large difference between σ_Π andσ_Σ, we must consider the steric effect on the electron exchange probability in the electron transfer processes 1 and 2. For this purpose, we calculate the electron density distribution of the 1π and 2π orbitals of CO and of the 4p atomic orbital of Kr by using the GAUSSIAN 98 ab initio program package with 6-311G (3df, 2pd) basis set. The electron exchange mechanism is schematically shown in Figure 4.

First, we consider the orbital overlap efficiency between the 2π orbital of CO and the 5s orbital of Kr in process 1 (ET). As shown in Figure 4, the lateral configuration is favorable for the orbital overlap, while the collinear configuration is unfavorable because the 5s orbital cannot efficiently interact with the 2π orbital that has a nodal plane along the C−O molecular axis.

Second, we consider the orbital overlap efficiency between the 1π orbital of CO and the unpaired 4p orbital of Kr in the process 2 (BET). For the Σ-configuration, the efficient overlap should be possible over a wide range of the impact parameter (b) region. Moreover, the efficient overlap between the set of orbitals, (4p + 1π) and (5s + 2π), requires that the 1π orbital must be in coplanar with the 2π orbital. For the Π-configuration, on the other hand, the efficient overlap between the unpaired 4p orbital and the 1π orbital forbids the efficient overlap between the 5s orbital and the 2π orbital at the relatively small impact

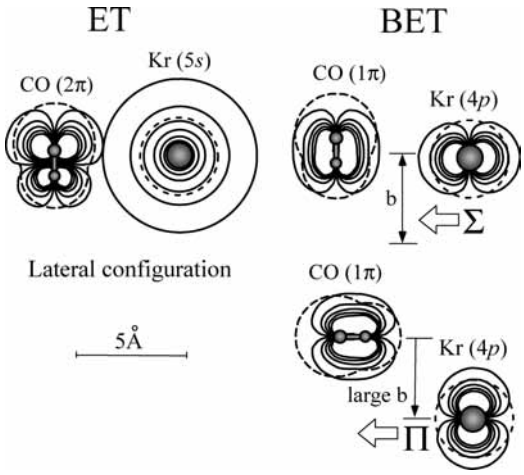

Figure 4. A schematic drawing of the energy transfer mechanism via the electron exchange. The electron density distributions of the 2π and 1π orbitals of CO and the 4p atomic orbital of Kr were calculated by using the GAUSSIAN 98 ab initio program package with 6-311G (3df, 2pd) basis set. Dashed lines indicate the van der Waals surface of molecule as an approximate position of the repulsive wall. The impact parameter was indicated by *b*. The lateral configuration is favorable for the orbital overlap between the 2π orbital of CO and the 5s orbital of Kr in process 1 (ET). For the Σ configuration, the efficient overlap between the 1π orbital of CO and the unpaired 4p orbital of Kr ($^3P_2$) should be possible at the relatively wide impact parameter *b* region. For the Π configuration, the favorable collision should be limited to the collision with the rather large impact parameter *b*.

parameter (*b*) region because the 5s orbital cannot efficiently interact with the 2π orbital that has a nodal plane along the C−O molecular axis. Therefore, the favorable collision at the Π-configuration should be limited within a narrow range of collision with the relatively large impact parameter. This large difference in the favorable impact parameter region between the Σ- and Π-configuration should cause the large difference in reactivity between σ_Σ and σ_Π. As a result, it is recognized that the observed atomic alignment effect qualitatively can be explained by the electron exchange mechanism.

The electron exchange mechanism can explain the difference in the cross section between CO ($a'\ ^3\Sigma^+$) and CO ($e^3\Sigma^-$) in a $(1\pi)^3\ (2\pi)^1$ configuration. The difference in the electron orbital configuration between CO ($a'\ ^3\Sigma^+$) and CO ($e^3\Sigma^-$) is that CO ($a'\ ^3\Sigma^+$) has the unpaired 1π and 2π electrons in the same plane (*xz* or *yz* plane) with the configuration of $(1\pi_x)^1\ (2\pi_x)^1$ or $(1\pi_y)^1\ (2\pi_y)^1$, whereas CO ($e^3\Sigma^-$) has the unpaired electrons in two different planes with the configuration of $(1\pi_x)^1\ (2\pi_y)^1$ or $(1\pi_y)^1\ (2\pi_x)^1$. The efficient overlap between the set of orbital, (4p + 1π) and (5s + 2π) inevitably leads to no formation of CO ($e^3\Sigma^-$) because the efficient overlap requires that the 1π orbital must be coplanar with the 2π orbital.

According to the similarity in the atomic alignment effect between CO (a') and CO*, it is suggested that the unassigned CO* should arise from the excited CO whose electron orbital configuration is similar to CO (a') (i.e., $(5\sigma)^2\ (1\pi)^3\ (2\pi)^1$). On the basis of efficient overlap between the set of orbital, (4p + 5σ) and (5s + 2π), the CO ($a\ ^3\Pi$) states in the $(5\sigma)^1\ (1\pi)^4\ (2\pi)^1$ configuration must show the different atomic alignment effect from CO (a') (i.e., σ_Π is expected to be larger than σ_Σ). From this point of view, it is unlikely that the CO* is the CO (a' and *d*) state with low vibrational levels formed from radiative decay of CO ($a\ ^3\Pi$: $v = 22$).[1] In the present study, the energetically accessible excited states of CO being in the $(5\sigma)^2\ (1\pi)^3\ (2\pi)^1$ configuration are the ($a'\ ^3\Sigma^+$, $e\ ^3\Sigma^-$, $d\ ^3\Delta$, $I\ ^1\Sigma^-$, $D\ ^1\Delta$) valence states. The possible involvement of the CO ($D\ ^1\Delta$) state might be expected for the CO* formation.

4. Conclusions

The atomic alignment effects for the formations of CO ($a'\ ^3\Sigma^+$), CO ($d\ ^3\Delta$), and CO* have been measured in the energy transfer reaction of oriented Kr ($^3P_2$) + CO. The emission intensities of CO ($a'\ ^3\Sigma^+$), CO ($d\ ^3\Delta$), and CO* are highly enhanced when the electron angular momentum of Kr ($^3P_2$) is aligned perpendicular to the relative velocity vector. The $|M_J'| = 2$ magnetic substate in the collision frame is significantly less reactive than the other M_J' states in every reaction channel. In addition, the large difference of the cross section between the Σ- and Π-configuration of the unpaired 4p orbital of Kr ($^3P_2$) is recognized for every reaction channels: $\sigma_\Sigma/\sigma_\Pi \approx 2.0$. The observed atomic alignment effects can be qualitatively explained in terms of both the M_J' dependent entrance surfaces being caused by the open shell character of the Kr^+ (^2P_j) ion core and the difference in the favorable impact parameter region for the efficient orbital overlap between the Σ- and Π-configuration. It is concluded that the observed atomic alignment effects support that the Kr ($^3P_2$) + CO reaction proceeds via the direct curve crossings between the entrance and exit covalent surfaces.

References and Notes

(1) Sadeghi, N.; Colomb, I.; Stoyanova, J.; Setser, D. W.; Zhong, D. *J. Chem. Phys.* **1995**, *102*, 2744.
(2) Tsuji, M.; Yamaguchi, K.; Nishimura, Y. *Chem. Phys.* **1988**, *123*, 151.
(3) Sobczynski, R.; Setser, D. W. *J. Chem. Phys.* **1991**, *95*, 3310.
(4) Tsuji, M.; Yamaguchi, K.; Obase, H.; Nishimura, Y. *Chem. Phys. Lett.* **1989**, *161*, 41.
(5) Tsuji, M.; Yamaguchi, K.; Yamaguchi, S.; Nishimura, Y. *Chem. Phys. Lett.* **1988**, *143*, 482.
(6) Velazco, J. E.; Kolts, J. H.; Setser, D. W. *J. Chem. Phys.* **1978**, *69*, 4357.
(7) Brewer, L.; Searcy, A. W. *Annu. Rev. Phys. Chem.* **1956**, *7*, 259.
(8) Watanabe, D.; Ohoyama, H.; Matsumura, T.; Kasai, T. *J. Chem. Phys.* **2006**, *125*, 084316.
(9) Watanabe, D.; Ohoyama, H.; Matsumura, T.; Kasai, T. *Phys. Rev. Lett.* **2007**, *99*, 043201.
(10) Aquilanti, V.; Grossi, G. *J. Chem. Phys.* **1980**, *73*, 1165.
(11) Aquilanti, V.; Candori, R.; Pirani, F.; Ottinger, Ch *Chem. Phys.* **1994**, *187*, 171.
(12) Aquilanti, V.; Linti, G.; Pirani, F.; Vecchiocative, F. *J. Chem. Soc., Faraday Trans. 2* **1989**, *85*, 955.
(13) Chiu, L. -Y. C.; Krümpelmann, T.; Ottinger, Ch. *Chem. Phys. Lett.* **1989**, *157*, 60.

JP907518U